

# Was GRB 990123 a unique optical flash?

Alicia M. Soderberg and Enrico Ramirez-Ruiz

*Institute of Astronomy, Madingley Road, Cambridge, CB3 0HA.  
ams, enrico@ast.cam.ac.uk*

## ABSTRACT

GRB 990123 was a long, complex gamma-ray burst accompanied by an extremely bright optical flash. We find different constraints on the bulk Lorentz of this burst to be consistent with the speculation that the optical light is emission from the reverse shock component of the external shock. Motivated by this currently favoured idea, we compute the prompt reverse shock emission to be expected for bursts in which multi-wavelength observations allow the physical parameters to be constrained. We find that for reasonable assumptions about the velocity of source expansion, a strong optical flash  $m_V \approx 9$  was expected from the reverse shocks, which were usually found to be mildly relativistic. The best observational prospects for detecting these prompt flashes are highlighted, along with the possible reasons for the absence of optical prompt detections in ongoing observations.

**Key words:** gamma-rays: bursts – stars: supernovae – X-rays: sources

## 1 INTRODUCTION

The discovery of a prompt and extremely bright optical flash in GRB 990123 (Akerlof et al. 1999), implying an apparent peak (isotropic) optical luminosity of  $5 \times 10^{49}$  erg s<sup>-1</sup>, has lead to widespread speculation that the observed radiation arose from the reverse shock component of the burst. The reverse shock propagates into the adiabatically cooled particles of the coasting ejecta, decelerating the shell particles and shocking the shell material with an amount of internal energy comparable to that of the material shocked by the forward shock. The typical temperature in the reverse-shocked fluid is, however, considerably lower than that of the forward-shocked fluid. Consequently, the typical frequency of the synchrotron emission from the reverse shock peaks at lower energy. It is believed to account for the bright prompt optical emission from GRB 990123. The reverse shock emission stops once the entire shell has been shocked and the reverse shock reaches the inner edge of the fluid. The ejecta cool adiabatically after the reverse shock has passed through and settle down into a part of the Blandford & McKee 1976 (BM) solution that determines the late profile of the decelerating shell and the external medium.

Given the importance of this prediction, we estimate the prompt reverse shock emission expected from bursts in which multi-frequency data has been able to constrain the burst physical parameters. We find a broad range of model parameters for which a strong optical flash is expected from most of these bursts. Unfortunately, no observations to search for an optical flash were performed for these cases. The possible reasons for the absence of detectable optical flux in other bursts are highlighted, along with the predic-

tions that may be useful for designing search strategies for the rapid follow up of optical flashes. Unlike the continuous forward shock, the hydrodynamic evolution of the reverse-shocked ejecta is more fragile. As we will demonstrate, the temperature of the reverse-shocked fluid is expected to be non-relativistic for most of these bursts and thus the evolution of their ejecta deviates from the BM solution. The detection of optical flashes, or firm upper limits, would play an important role in discriminating between *cold* and *hot* shell evolution. Moreover, the strong dependence of the peak time of this optical flash on the bulk Lorentz factor  $\Gamma$  provides a way to estimate this elusive parameter. We discuss how different constraints on  $\Gamma_0$  for GRB 990123 are consistent with optical emission from the reverse shock. We assume  $H_0 = 65$  km s<sup>-1</sup> Mpc<sup>-1</sup>,  $\Omega_M = 0.3$ , and  $\Omega_\Lambda = 0.7$ .

## 2 THE ROLE OF $\Gamma$

Relativistic source expansion plays a crucial role in virtually all current GRB models (Piran 1999; Mészáros 2001). The Lorentz factor is not, however, well determined by observations. The lack of apparent photon-photon attenuation up to  $\approx 0.1$  GeV implies only a lower limit  $\Gamma \approx 30$  (Mészáros, Laguna & Rees 1993), while the observed pulse width evolution in the gamma-ray phase eliminates scenarios in which  $\Gamma \gg 10^3$  (Lazzati et al. 1999; Ramirez-Ruiz & Fenimore 2000). The initial Lorentz factor is set by the baryon loading, that is  $m_0 c^2$ , where  $m_0$  is the mass of the expanding ejecta. This energy must be converted to radiation in an optically-thin region, as the observed bursts are non-thermal. The radius of transparency of the ejecta is

$$R_\tau = \left( \frac{\sigma_T E}{4\pi m_p c^2 \Gamma_0} \right)^{1/2} \approx 10^{12} - 10^{13} \text{ cm}, \quad (1)$$

where  $E$  is the isotropic equivalent energy generated by the central site. The highly variable  $\gamma$ -ray light curves can be understood in terms of internal shocks produced by velocity variations within the relativistic outflow (Rees & Mészáros 1994). In an unsteady outflow, if  $\Gamma$  were to vary by a factor of  $\approx 2$  on a timescale  $\delta T$ , then internal shocks would develop at a distance  $R_i \approx \Gamma^2 c \delta T \geq R_\tau$ . This is followed by the development of a blast wave expanding into the external medium, and a reverse shock moving back into the ejecta. The inertia of the swept-up external matter decelerates the shell ejecta significantly by the time it reaches the deceleration radius (Mészáros & Rees 1993),

$$R_d = \left( \frac{E}{n_0 m_p c^2 \Gamma_0^2} \right)^{1/3} \approx 10^{16} - 10^{17} \text{ cm}. \quad (2)$$

Given a certain external baryon density  $n_0$ , the initial Lorentz factor then strongly determines where both internal and external shocks develop. Changes in  $\Gamma_0$  will modify the dynamics of the shock deceleration and the manifestations of the afterglow emission.

### 3 REVERSE SHOCK EMISSION AND $\Gamma_0$

It has been predicted that the reverse shock produces a prompt optical flash brighter than 15th magnitude with reasonable energy requirements of no more than a few  $10^{53}$  erg emitted isotropically (Mészáros & Rees 1999; Sari & Piran 1999a; hereinafter MR99 and SP99). The forward shock emission is continuous, but the reverse shock terminates once the shock has crossed the shell and the cooling frequency has dropped below the observed range. The reverse shock contains, at the time it crosses the shell, an amount of energy comparable to that in the forward one. However, its effective temperature is significantly lower (typically by a factor of  $\Gamma$ ). Using the shock jump conditions and assuming that the electrons and the magnetic field acquire a fraction of the equipartition energy  $\varepsilon_e$  and  $\varepsilon_B$  respectively, one can describe the hydrodynamic and magnetic conditions behind the shock.

The reverse shock synchrotron spectrum is determined by the ordering of three break frequencies, the self-absorption frequency  $\nu_a$ , the cooling frequency  $\nu_c$  and the characteristic synchrotron frequency  $\nu_m$ , which are easily calculated by comparing them to those of the forward shock (MR99; SP99; Panaiteescu & Kumar 2000). The equality of energy density across the contact discontinuity suggests that the magnetic fields in both regions are of comparable strength.

Assuming that the forward and reverse shocks both move with a similar Lorentz factor, the reverse shock synchrotron frequency is given by

$$\nu_m = 5.840 \times 10^{13} \epsilon_{e,-1}^2 \epsilon_{B,-2}^{1/2} n_{0,0}^{1/2} \Gamma_{0,2}^2 (1+z)^{-1/4} \text{ Hz}, \quad (3)$$

while the cooling frequency  $\nu_c$  is equal to that of the forward shock. Here we adopt the convention  $Q = 10^x Q_x$  for expressing the physical parameters, using cgs units. The spectral power  $F_{\nu_m}$  at the characteristic synchrotron frequency is

$$F_{\nu_m} = 4.17 D_{28}^{-2} \epsilon_{B,-2}^{1/2} E_{53} n_{0,0}^{1/2} \Gamma_{0,2} (1+z)^{3/8} \text{ Jy}. \quad (4)$$

The distribution of the injected electrons is assumed to be a power law of index  $-p$ , above a minimum Lorentz factor  $\gamma_i$ . For an adiabatic blast wave, the corresponding spectral flux at a given frequency above  $\nu_m$  is  $F_\nu \approx F_{\nu_m} (\nu/\nu_m)^{-(p-1)/2}$ , while below  $\nu_m$  is characterised by a synchrotron tail with  $F_\nu \approx F_{\nu_m} (\nu/\nu_m)^{1/3}$ . Similar relations to those found for a radiative forward shock hold for the reverse shock (Kobayashi 2000; hereinafter K00).

Unlike the synchrotron spectrum, the afterglow light curve at a fixed frequency strongly depends on the hydrodynamics of the relativistic shell, which determines the temporal evolution of the break frequencies  $\nu_m$  and  $\nu_c$ . The forward shock is always highly relativistic and thus is successfully described using the relativistic generalisation of theory of supernova remnants. In contrast, the reverse shock can be mildly relativistic. In this regime, the shocked shell is unable to heat the ejecta to sufficiently high temperatures and its evolution deviates from the BM solution (Kobayashi & Sari 2000; hereinafter KS00). Shells satisfying

$$\xi \approx 0.01 E_{52}^{1/6} \Delta_{11}^{-1/2} \Gamma_{0,2}^{-4/3} n_{0,1}^{-1/6} > 1, \quad (5)$$

are likely to have a Newtonian reverse shock\*, otherwise the reverse shock is relativistic and it considerably decelerates the ejecta. The width of the shell,  $\Delta$ , can be inferred directly from the observed burst duration by  $\Delta = c T_{\text{dur}} / (1+z)$  assuming the shell does not undergo significant spreading (Piran 1999).

If  $\xi > 1$ , then the reverse shock is in the sub-relativistic temperature regime for which there are no known analytical solutions. In order to constrain the evolution of  $\Gamma$  in this regime it is common to assume  $\Gamma \propto R^{-g}$  where  $3/2 \leq g \leq 7/2$  (MR99; KS00). For an adiabatic expansion,  $\Gamma \propto T^{-g/(1+2g)}$  and so  $\nu_m \propto T^{-3(8+5g)/(7(1+2g))}$  and  $F_{\nu_m} \propto T^{-(12+11g)/(7(1+2g))}$ . The spectral flux at a given frequency expected from the reverse shock gas drops then as  $T^{-(2+3g)/(7(1+2g))}$  below  $\nu_m$  and  $T^{-(7+24p+15pg)/(14(1+2g))}$  above. For a typical spectral index  $p = 2.5$ , the flux decay index varies in a relatively narrow range ( $\approx 0.4$ ) between limiting values of  $g$ .

### 4 CONSTRAINTS ON THE $\Gamma_0$ OF GRB 990123

Despite ongoing observational attempts, the optical flash associated with GRB 990123 remains the only event of its kind detected to date. Observations of this optical flash appear to be in good agreement with early predictions for the reverse shock emission (Sari & Piran 1999b). As a result, numerous studies have been done on this event in which reverse shock theory has been applied to burst observations in order to constrain physical parameters and burst properties, including  $\Gamma_0$ . Current estimates on the bulk Lorentz factor for GRB 990123 stretch over nearly an order of magnitude, with values ranging from  $\approx 200$  (SP99) to  $\approx 1200$  (Wang, Dai & Lu 2000). It should be noted, however, that these

\* It should be remarked that equations (3) and (4) refer to this reverse shock regime. Equations for the relativistic case are relatively similar, the biggest discrepancy being that the peak flux is inversely proportional to  $\Gamma$  (see equations (7)-(9) of K00).

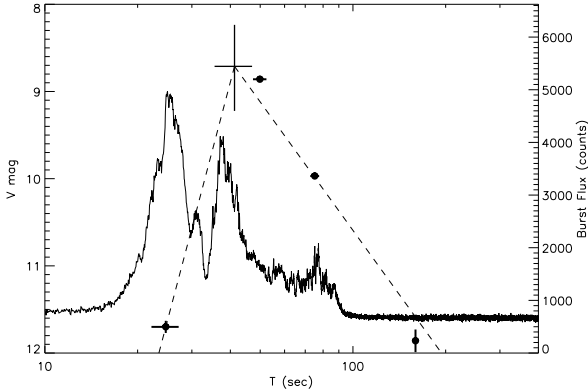


**Figure 1.** BATSE and ROTSE light curves for GRB 990123 as a function of time from the BATSE trigger. Dashed lines represent theoretical predictions for the rise  $\propto T^{3p-3/2}$  and decay  $\propto T^{-(21+73p)/96}$  of an adiabatic reverse shock light curve, assuming the shell is thin and cooling slowly. We predict that the optical flash peaked  $\approx 41 \pm 6$  seconds after the trigger.

estimates were made before accurate burst parameters for GRB 990123 were known, and consequently they include approximations and parameters from other GRB afterglows.

By fitting multi-frequency afterglow light curves, physical parameters for 8 GRBs have recently been reported (Panaitescu & Kumar 2001a, hereinafter PK01). Best fit values presented for GRB 990123 are  $E_{j,51} = 1.5^{+3.3}_{-0.4}$  (initial jet energy),  $\theta_0 = 2.1^{+0.1}_{-0.9}$ ,  $n_{0,-3} = 1.9^{+0.5}_{-1.5}$ ,  $\epsilon_{e,-2} = 13^{+1}_{-4}$ ,  $\epsilon_{B,-4} = 7.4^{+23}_{-5.9}$ , and  $p = 2.28^{+0.05}_{-0.03}$  with a rough estimate for the bulk Lorentz factor of  $\Gamma_0 = 1400 \pm 700$  (PK01). Using these physical parameters, we present a comprehensive examination of the constraints on  $\Gamma_0$  and report a best-fit value based on an analysis of these constraints.

Observational estimates for the time of peak flux enabled a measurement of the initial Lorentz factor with reasonable accuracy using the physical parameters specific to GRB 990123. Assuming the optical flash was the result of the reverse shock, the initial bulk Lorentz factor

$$\Gamma_0 = 237 E_{52}^{1/8} n_{0,0}^{-1/8} T_{d,1}^{-3/8} (1+z)^{3/8} \quad (6)$$

where  $T_d$  is the time of peak flux in the observer frame. Light curves for the optical flash and  $\gamma$ -ray emission are shown in Figure 1. Dashed lines represent theoretical predictions for the rise  $\propto T^{3p-3/2}$  and decay  $\propto T^{-(21+73p)/96}$  of an adiabatic reverse shock light curve, assuming the shell is thin, i.e.  $\Delta < (E/(2n_0 m_p c^2 \Gamma_0^8))^{1/3}$ , and cooling slowly (K00). Using the recently reported physical parameters, one finds GRB 990123 to have a marginal thickness, as predicted by K00. The observed rise time is, however, in good agreement with that of a thin shell  $\approx T^{5.5}$  (in contrast with  $\approx T^{1/2}$  for a thick shell). The shape of the light curve is determined by the time evolution of the three spectral break frequencies, which in turn depend on the hydrodynamical evolution of the fireball. In the case of GRB 990123, the typical synchrotron frequency  $\nu_m = 1.5 \times 10^{14}$  Hz is well below the cooling frequency  $\nu_c = 1.0 \times 10^{19}$  Hz, and therefore places the burst in a regime with a flux decay governed by the relation  $F_\nu \propto T^{-(21+73p)/96}$ . This implies a decay of  $\approx T^{-2}$  for the optical flash of GRB 990123. Applying these light curve predictions to the prompt optical data and taking observa-

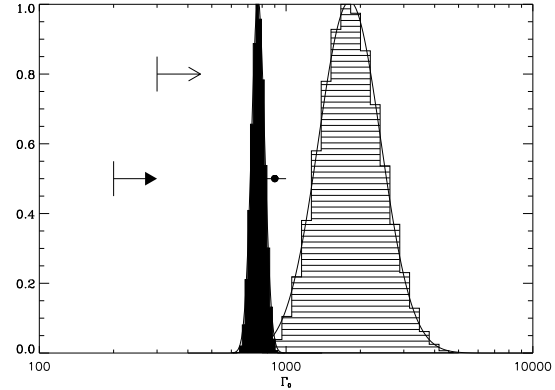


**Figure 2.** Collective constraints on  $\Gamma_0$  for GRB 990123. These include estimates from the burst kinematics (narrow distribution), synchrotron spectral decay (wider distribution), prompt emission pulse width (filled arrow), and jet modelling (unfilled arrow). We find a best fit value of  $\Gamma_0 = 900 \pm 100$ .

tional uncertainties as well as burst parameter uncertainties into account, we predict that the optical flash peaked  $T_{\text{peak}} \approx 41 \pm 6$  s after the GRB started. Substitution for  $T_{\text{peak}}$  in equation (6) gives  $\Gamma_0 = 770 \pm 50$ .

Observations of the optical peak brightness enable further accurate constraints on the value of  $\Gamma_0$ . The synchrotron spectrum from relativistic electrons comprises four power-law segments, separated by three critical frequencies. The prompt optical flash in GRB 990123 is observed at a frequency that falls well below the cooling frequency, but above the typical synchrotron frequency:  $\nu_a < \nu_m < \nu_{\text{obs}} < \nu_c$ . The synchrotron spectrum for this spectral segment is given by  $F_{\text{obs}} = F_{\nu_m} (\nu_{\text{obs}}/\nu_m)^{(p-1)/2} (1+z)^{1/2-p/8}$  where  $\nu_{\text{obs}}$  is taken to be the ROTSE optical frequency. Assuming the optical peak flux  $F_{\text{obs}}$  observed in GRB 990123 is radiation arising from the reverse shock, we find  $\Gamma_0 = 1800^{+600}_{-500}$ .

Although observations of a reverse shock induced optical peak enable fairly accurate calculations of the bulk Lorentz factor, it remains possible to obtain information on  $\Gamma_0$  in situations when an optical flash has not been detected. Consider an internal shock which produces an instantaneous burst of isotropic  $\gamma$ -ray emission at a time,  $t$ , and radius,  $R_i$ , in the frame of the central engine. The kinematics of colliding shells implies that although photons are emitted simultaneously, the curvature of the emitting shell spreads the arrival time of the emission over a period of  $\Delta T_p$ , thereby producing the observed width in individual pulses. The delay in arrival time between on-axis photons and those at  $\theta \approx \Gamma^{-1}$  is a function of the radius of emission and the Lorentz factor according to:  $\Delta T_p/(1+z) = R_i/(2c\Gamma^2)$  where  $\Gamma = \Gamma_0$  in the early phase of the expansion (Fenimore, Madras & Nayashin 1996). In order to allow photons to escape,  $R_i$  must be larger than the radius of transparency  $R_\tau$ . This imposes a lower limit on the initial bulk Lorentz factor such that:  $\Gamma_0 > (R_\tau/2c\Delta T_p)^{1/2} (1+z)^{1/2}$ . We determine  $\Delta T_p$  for GRB 990123 by measuring the average pulse width through autocorrelation methods based on those described in Fenimore, Ramirez-Ruiz & Wu (1999) and find  $\Delta T_p \approx 0.45$  s. Using the burst parameters to estimate  $R_\tau$  from equation (1) and applying the inequality relation defined above, we find a lower limit of  $\Gamma_0 > 200$ . Figure 2 displays the collec-

tive constraints on  $\Gamma_0$  for GRB 990123. An additional lower limit of  $\Gamma_0 > 300$  constraint from afterglow modelling is also included (Kumar & Panaiteescu 2001b). The combination of these constraints leads to an average bulk Lorentz factor for GRB 990123 of  $\Gamma_0 = 900 \pm 100$  and thus  $R_\tau \approx 1.3 \times 10^{14}$ .

## 5 GRB 991023: A UNIQUE OPTICAL FLASH?

Throughout the two years since its discovery, the optical flash associated with GRB 990123 has provoked continuous study in order to determine whether it was consistent with current reverse shock theory. More importantly, if it can be proven that this optical flash was the result of a typical reverse shock event, then we need to understand why it is the only event detected to date. Important information may be gained by estimating the prompt reverse shock emission expected from bursts with known physical parameters. In our analysis, we use all 7 bursts from PK01 with secure redshifts: 990123; 990510; 991208; 991216; 000301c; 000926; 010222. Reverse shock analytic light curves were derived for each of the bursts to produce a set of predicted optical flash spectra given various values of the bulk Lorentz factor. Figure 3 displays the reverse shock peak spectra predicted for the sub-relativistic regime ( $\Gamma_0 = 10^2$ , upper panel) and the relativistic regime ( $\Gamma_0 = 10^3$ , lower panel). The mildly-relativistic reverse shock spectrum for GRB 990123 is included in both panels assuming our best fit value of  $\Gamma_0 = 900$ . The visible ROTSE spectral range is displayed in the upper panel, while the multi-frequency bands of *Swift* are shown in the lower panel. It is critical to note that the *only* optical flash which has been successfully detected (GRB990123, solid thick line) has one of the *lowest* predicted optical fluxes. If it is assumed that the six GRBs did in fact produce optical flashes resulting from reverse shocks, then it is clear that their non-detection was not due to comparably low peak fluxes. Unfortunately, no early observations were performed for this set of bursts. Moreover, the predicted reverse shock emission is too faint in X-rays to be detected along with the prompt  $\gamma$ -ray emission.

Kehoe et al. (2001) reported non detections of the optical flashes for six GRBs with localisation errors of  $1 \text{ deg}^2$  or better. One possible explanation for these non-detections, apart from both positional uncertainties and lack of deep imaging<sup>†</sup>, could be related to the time at which the optical flash reached its maximum brightness. It is clear that the time at which the reverse shock emission peaks plays an important role in the ability to detect a prompt optical flash. Current instruments aimed at detecting flashes are limited by their response times, often  $\approx 10$  seconds after the initial trigger (Akerlof et al. 1999). Consequently, there exists the possibility that a significant fraction of optical flashes peak before images were taken. The peak time can be estimated with  $T_{\text{peak}} = \max[T_d, \Delta/c]$ . The time of the peak in the the reverse shock emission is shown as a function of  $\Gamma_0$  in Fig. 4, along with the lower limits on the bulk Lorentz

<sup>†</sup> K00 found that the ROTSE limits in at least two of these bursts (GRB 981121 and GRB 981223) does not give strong constraints and the lack of detections can easily be explained either by invoking a lower  $n_0$  or if  $\Gamma_0$  slightly deviates from that of GRB 990123.

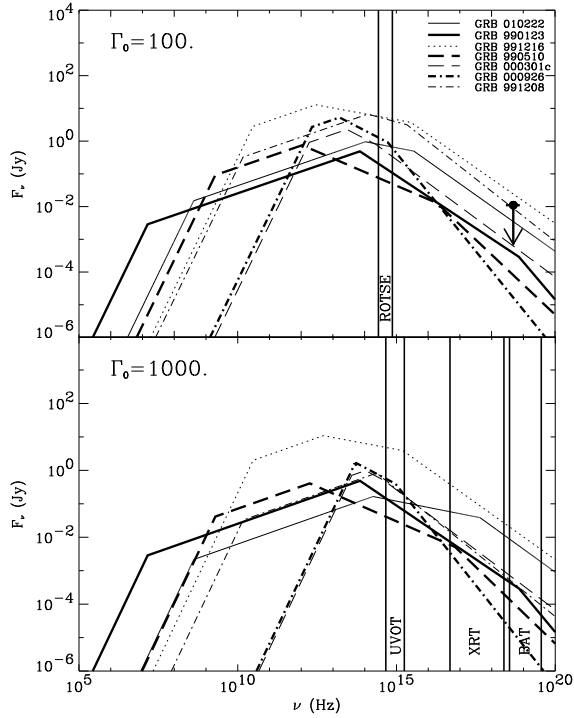


**Figure 3.** Estimates of reverse shock peak emission for bursts with known physical parameters. The two values of  $\Gamma_0$  portray the two relativistic regimes. The reverse shock spectrum for GRB 990123 assumes our best fit value of  $\Gamma_0 = 900$ . Observed SAX/WFC flux for the 990123  $\gamma$ -ray trigger appears in the upper panel. ROTSE spectral window and *Swift* multi-frequency bands are shown in the upper and lower panels respectively.

factor reported by Panaiteescu & Kumar (2001b). We find that for reasonable values values of  $\Gamma_0 \approx 10^2 - 10^3$ , 50 per cent of the optical flashes would have peaked before GRB 990123 and the rest within 3 minutes of their initial trigger.

Another possible explanation for these non-detections involves the hydrodynamical evolution of the reverse shock. If the reverse shock is only mildly relativistic ( $\xi \approx 1$ ), then it cannot heat the ejecta to sufficiently high temperatures and so the Blandford-McKee solution is not valid (KS00). Since the flux brightness and photon energy are both directly proportional to  $\Gamma$ , determining whether the burst is relativistic constrains the flux decay. Therefore, to understand and detect GRB flashes, we should examine whether events go undetected due to the behaviour of the Lorentz factor decay. Using PK01 physical parameters and equation (5), we calculate  $\xi$  for GRB 990123 and six additional bursts for which there was no detected optical flash. Figure 4 (upper panel) displays the dependence of  $\xi$  on  $\Gamma_0$  for each burst. Unsurprisingly, we find that the reverse shock in GRB 990123 is mildly relativistic with  $\xi = 1.0 \pm 0.1$ , which supports the early prediction that  $\xi = 0.7$  made by KS00, who stated that the value could in fact be larger. The reverse shock in most of these bursts was expected to be mildly relativistic for  $\Gamma_0 \leq 500$ . The hydrodynamics of the *cold* shocked ejecta is very different from that of the *hot* ejecta which is described by the BM76 solution. Surprisingly, both cases predict rather similar light curves (KS00), with decay laws that vary in relatively narrow ranges. Hence, it is unlikely

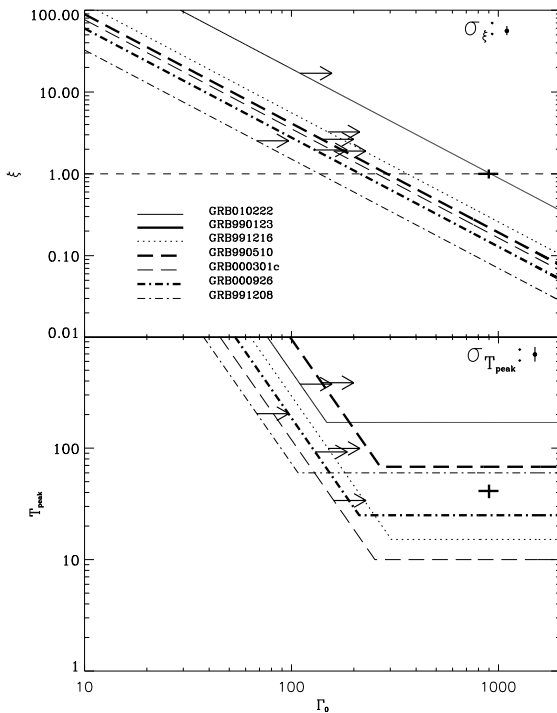


**Figure 4.** Estimates of  $\xi$  and  $T_{\text{peak}}$  for GRBs with available multi-frequency data. For reasonable values of  $\Gamma_0 \approx 10^2 - 10^3$ , we find that: (i) the reverse shock in most cases was expected to be mildly relativistic with  $\xi \approx 1$  (upper panel); (ii) 50 per cent of these bursts reached peak emission before GRB 990123 with the rest within 3 minutes of their initial trigger (lower panel).

that the non-detection of optical flashes is linked to the relativistic regime of their reverse shock.

The absence of detectable optical flux accompanying a strong  $\gamma$ -ray emission may simply be due to dust obscuration. Because GRBs represent the final phase of the evolution of massive stars (MacFadyen & Woosley 1999) which do not live long enough to leave their birth place, a large fraction are likely to be still enshrouded in their placental clouds (Blain & Natarajan 2000). This environment will strongly attenuate the optical afterglow radiation (Waxman & Draine 2000, Venemans & Blain 2001, Ramirez-Ruiz, Trentham & Blain 2001). The optical observations of GRB late afterglows are consistent with this picture: 50-70 per cent of all bursts have no optical counterpart down to  $R=24$ , which implies a minimum absorption of  $A_R \approx 2$  (Lazzati, Covino & Ghisellini 2001; Reichart & Yost 2001).

## 6 OBSERVATIONAL PROSPECTS AND CONCLUSIONS

An obvious question becomes: how is it that the optical flash associated with GRB 990123 remains the only event of its kind detected to date? Observations of both faint and heavily dust-enshrouded optical flashes could be missing due to the capability of current instruments. With the launch of *Swift*, the facilities necessary to detect reverse shock emission will be made readily available. Within 20-70 seconds of the initial trigger, the UV and optical telescope (UVOT)

will begin collecting images of the burst down to  $B=24$ . We have predicted that optical flashes brighter than  $m_V \approx 9$  for at least a subset of bursts, with typical peak times of  $\approx 50$  seconds and peak frequencies of  $\approx 10^{15}$  Hz. However, there exist necessary limitations to our approach: we assumed that the equipartition parameters are the same across the contact discontinuity, and we have used only a subset of bursts bearing relatively bright optical afterglows. A more detailed analysis of the underlying reasons for the non-detections of prompt optical afterglows will require the large and unbiased sample of *Swift* GRB afterglows.

In summary, we show that reverse shocks are likely to produce strong optical flashes in most GRBs, and that dust obscuration seems to be the most likely reason for their non-detection. If reverse shock emission turns out to be insignificant, then the explanation for the bright optical flashes will surely be even more remarkable and fascinating.

## ACKNOWLEDGEMENTS

We thank A. Blain, D. Lazzati, M. J. Rees and E. Rossi for helpful conversations. AMS was supported by the NSF GRFP. ER-R thanks CONACYT, SEP and the ORS for support.

## REFERENCES

- Akerlof C. W. et al., 1999, Nature, 398, 400
- Blain A. W., Natarajan P., 2000, MNRAS, 312, L35
- Blandford R. D., McKee C. F., 1976, Phys. Fluids, 19, 1130 (BM)
- Fenimore E. E., Madras C. D., Nayakshin S., 1996, ApJ, 473, 998
- Fenimore E. E., Ramirez-Ruiz E., Wu B., 1999, ApJ, 518, L73
- Kehoe, R. et al., 2001, ApJ, 554, L159
- Kobayashi S., 2000, ApJ, 545, 807 (K00)
- Kobayashi S., Sari R., 2000, ApJ, 542, 819 (KS00)
- Lazzati D., Ghisellini G., Celotti, A., 2001, MNRAS, 309, L13
- Lazzati D., Campana S., Ghisellini G., 2001, MNRAS submitted (astro-ph/0011443)
- MacFadyen A. I. & Woosley S. E., 1999, ApJ, 524, 262.
- Mészáros P., 2001, Science, 291, 79
- Mészáros P., Rees M. J., 1993, ApJ, 405, 278
- Mészáros P., Laguna P., Rees M. J., 1993, ApJ, 415, 181
- Mészáros P., Rees M. J., 1999, MNRAS, 306, L39 (MR99)
- Panaiteescu A., Kumar P., 2000, ApJ, 543, 66
- Panaiteescu A., Kumar P., 2001a, ApJ, 560, L53 (PK01)
- Panaiteescu A., Kumar P., 2001b, ApJ submitted (astro-ph/0109124)
- Piran, T., 1999, Physics Reports, 314, 575
- Ramirez-Ruiz E., Fenimore E. E., 2000, ApJ, 539, 712
- Ramirez-Ruiz E., Trentham N., Blain A., 2001, MNRAS submitted (astro-ph/0103239)
- Rees M. J., Mészáros P., 1994, ApJ, 430, L93
- Reichart D. E., Yost S. A., 2001, ApJ submitted (astro-ph/0107545)
- Sari R., Piran T., 1999a, ApJ, 517, L109 (SP99)
- Sari R., Piran T., 1999b, ApJ, 520, 641
- Venemans B. P., Blain A. W., 2001, MNRAS, 325, 1477
- Wang X. Y., Dai Z. G., Lu T., 2000, MNRAS, 319, 1159
- Waxman E., Draine B. T., 2000, ApJ, 537, 796

This paper has been produced using the Royal Astronomical Society/Blackwell Science L<sup>A</sup>T<sub>E</sub>X style file.